LUMINOSITY SEGREGATION FROM MERGING IN CLUSTERS OF GALAXIES

R. FUSCO-FEMIANO
Istituto di Astrofisica Spaziale CNR, via Enrico Fermi 21/23, CP 67, I-00044 Frascati, Italy

AND

N. MENCI
Osservatorio Astronomico di Roma, via Osservatorio, 00040 Monteporzio, Italy

ABSTRACT

We compute the evolution of the space-dependent mass distribution of galaxies in clusters that arise from binary aggregations by solving a space-dependent Smoluchowski equation. From the solutions, we derive the distribution of intergalactic distances for different ranges of mass (and corresponding magnitudes). We compare the results with the observed distributions and find that the different degrees of luminosity segregation observed in clusters are well accounted for by our merging model. In addition, the presence of luminosity segregation is related to dynamical effects that also show up in different but connected observables, such as galaxy velocity profiles that decrease toward the center and X-ray–measured β-parameters smaller than 1. We predict that both luminosity segregation and the observables above (being a product of binary aggregations) are inversely correlated with the core radius and with the galaxy velocity dispersion; we also discuss how the whole set of predictions compares with up-to-date observations.

Subject headings: galaxies: clusters: general — galaxies: distances and redshifts — intergalactic medium

1. INTRODUCTION

The dynamical evolution of galaxy clusters is currently believed to go through two major phases. In the first phase, usually referred to as violent relaxation (Lynden-Bell 1967), the evolution is controlled by a collective potential and results in a Maxwell velocity distribution of galaxies; in the second phase, the dynamics is dominated by two-body processes, and binary collisions (both elastic and inelastic) drive the evolution. In fact, in this latter phase for ordinary galaxy sizes and separations the collision timescale is much less than the Hubble time.

Although a complete theoretical description of the two-body phase of dynamical evolution of clusters is still lacking, observations, N-body simulations, and computations based on statistical methods (Monte Carlo and Fokker-Planck simulations) have combined to shed light on many dynamical properties of clusters in this stage. These properties are characterized by a large cluster-to-cluster variance, and include the presence of a *velocity bias*, $b_v^2 = \langle v^2 \rangle / \sigma^2 < 1$, of the galaxy velocity dispersion $\langle v^2 \rangle^{1/2}$ with respect to the dark matter's σ (see N-body simulations of Carlberg & Dubinski 1991; Evrard, Summers, & David 1994; Katz & White 1993; Carlberg 1994; Summers, Davis, & Evrard 1995); galaxy *velocity dispersion profiles that decrease toward the cluster center* (see observations by Kent & Sargent 1983; Sharples, Ellis, & Gray 1988; Girardi et al. 1996); and *mass segregation*, i.e., the tendency for more massive galaxies to be located near the cluster center (see simulations by Roos & Aarseth 1982; Farouki, Hoffman, & Salpeter 1983), with the associated luminosity segregation (observed in several clusters; see Rood et al. 1972; Oemler 1974; White 1977; Dressler 1978; Quintana 1979; Sarazin 1980; Kent & Gunn 1982; Oegerle, Hoessel, & Ernst 1986; Binggeli, Tammann, & Sandage 1987; Dominguez-Tenreiro & del Pozo-Sanz 1992; Stein 1996).

Because of the large variance observed in the above effects, appreciable uncertainties exist about their dependence on the characteristics of the system, although a general trend of larger effects for smaller clusters might be inferred from the data when only relaxed clusters (with no prominent substructure or asphericity) are considered.

A complete description of the postvirialization phase of galaxy clusters should be able to connect all the above effects and to explain the observed variance in terms of dynamical properties of clusters. In previous papers (Fusco-Femiano & Menci 1995, hereafter Paper I; Menci & Fusco-Femiano 1996, hereafter Paper II), we showed that the loss of kinetic energy in inelastic galaxy collisions (binary aggregations) in clusters with $\sigma \lesssim 900$ km s^{-1} can significantly change the velocity distribution of galaxies. The model not only simultaneously accounts for the velocity bias and for centrally decreasing velocity dispersion profiles, but also predicts a correlation of such effects with the shape (the core radius) and the depth (the dark matter velocity dispersion) of the cluster potential wells, in good agreement with observations. In addition, the aggregation model can successfully connect the above dynamical effects to other observed properties of galaxy clusters (Paper I), such as the β-parameter (expressing the ratio of the galaxy orbital specific energy to the specific energy of the X-ray–emitting plasma) and the Butcher-Oemler effect (see Cavaliere & Menci 1993).

Thus, aggregations seem to constitute a leading mechanism in the postvirialization phase of clusters with velocity dispersions of $\lesssim 900$ km s^{-1}, while in larger clusters they are highly suppressed as a result of the large galaxy relative velocities (see numerical results of Richstone & Malmuth 1983). To further assess the role of galaxy merging in the two-body dynamical phase, we here address the problem of luminosity segregation (hereafter LS). This is expected to be generated when aggregations are effective, since merging builds up larger galaxies mainly in the central regions, where the larger density favors binary aggregation. Thus we extend our treatment of galaxy inelastic collisions, based on the solution of a collisional Boltzmann-Liuoville equation, to include position-dependent mass spectra of interacting galaxies. The predictions of our

model will be compared with observational results, focusing on the correlation of the segregation effects with properties of clusters such as richness, density distribution, and velocity dispersion. Finally, we shall show how the merging model connects LS with the dynamical effects discussed above and with their X-ray counterparts.

The paper is organized as follows. In § 2 we discuss the collisional Boltzmann equation and describe our solutions for the evolution of the position-dependent mass distribution. In § 3.1 we describe the standard method we use for the comparison with the data, based on the autocorrelation function for galaxies of different mass. The comparison is performed in § 3.2. Section 4 is devoted to a discussion and conclusions.

2. RADIUS-DEPENDENT MASS DISTRIBUTION FROM BINARY AGGREGATIONS

2.1. The Boltzmann Equation for Merging Galaxies

The evolution with time t of the distribution $f_t(M, r, v)$ of interacting galaxies with velocity v and mass M at the position r inside the gravitational potential ψ of a cluster can be described by the collisional Boltzmann equation. Assuming spherical symmetry, the latter can be written in spherical coordinates $r = (r, \theta, \phi)$ and $v = (v_r, v_\theta, v_\phi)$ for the distribution $f(M, r, v_r, v_t)$, as follows (see, e.g., Saslaw 1985):

$$\partial_t f_t(M, r, v_r, v_t) + v_r \frac{\partial f_t(M, r, v_r, v_t)}{\partial r} + \left(\frac{v_t^2}{r} - \frac{\partial \psi}{\partial r}\right) - 2\frac{v_r v_t^2}{r}\frac{\partial f_t(M, r, v_r, v_t)}{\partial v_t^2}$$

$$= \frac{1}{2}\int_0^M dM' \int_{-\infty}^\infty dv_r' \int_0^\infty dv_t'^2 f_t(M', r, v_r', v_t') f_t(M - M', r, v_r'', v_t'')\Sigma(M', M - M', v_{\rm rel})v_{\rm rel}$$

$$- \int_0^\infty dM' \int_{-\infty}^\infty dv_r' \int_0^\infty dv_t'^2 f_t(M, r, v_r, v_t) f_t(M', r, v_r', v_t')\Sigma(M', M', v_{\rm rel})v_{\rm rel} , \quad (1)$$

where $v_t^2 \equiv v_\theta^2 + v_\phi^2$ is the square tangential component of velocity, and the gravitational cross section for interactions Σ depends on the relative velocity $v_{\rm rel} \equiv v' - v''$. The velocity v'' in the first integral in equation (1) is related to v and v' by the requirement of momentum conservation, $M'v' + (M - M')v'' = Mv$. Here we assume that the galaxies do not gain or loose mass via processes other than merging. To obtain a fully self-consistent description, equation (1) should be complemented with the Poisson equation for the gravitational potential ψ, with a source term $\int dM dv_r dv_t^2 f_t(M, r, v_r, v_t)$, which includes the galaxy distribution itself. However, since we are interested in the postvirialization phase of cluster evolution, where the potential is essentially fixed, we shall assume a King potential $\psi(r)$ and follow the evolution of the galaxy mass distribution at different radii.

Since our aim is to probe the effectiveness of interaction in producing mass segregation, we introduce some approximations (a discussion of them is given in the final section). First, we assume the velocity distribution to be independent of the mass and of the spatial distribution of galaxies, so that the distribution in equation (1) can be factorized into a velocity distribution $p(v)$ and a position-dependent mass distribution $N(M, r, t)$. Such an approximation does not actually hold (see Paper I), but, as we discuss in the final section, for our purpose in the present paper it is a *conservative* assumption. Second, we assume that the radial and tangential velocity distributions are mutually independent and both normally distributed. In this case, integration of equation (1) over velocities leads to the following position-dependent Smoluchowski equation:

$$\partial_t N(M, r, t) = \frac{1}{2}\int dM' N(M', r, t)N(M - M', r, t)\langle\Sigma(M', M - M')v_{\rm rel}\rangle$$

$$- \int dM' N(M, r, t)N(M', r, t)\langle\Sigma(M, M')v_{\rm rel}\rangle , \quad (2)$$

where the average is over the velocity distribution.

The cross section is given by (Saslaw 1985): $\Sigma(M, M') = \epsilon(v_{\rm rel}/v_g)\pi(r^2 + r'^2)(1 + v_g^2/v_{\rm rel}^2)$, where r and r' are the radii of the interacting galaxies (proportional to $M^{2/3}$) and $v_g \propto G(M + M')/R$ is the escape velocity at closest approach, $R \approx (r + r')$. The efficiency ϵ is determined from N-body results (see Richstone & Malmuth 1983) and is zero when $v_{\rm rel} \gtrsim 3v_g$, so that aggregations are highly suppressed in very rich clusters. It is convenient to express all quantities in terms of the *adimensional* mass $m \equiv M/M_*$, normalized to the characteristic mass M_* (which corresponds to a galaxy with characteristic luminosity L_*). From $r \sim (M/\rho)^{1/3}$, the relation $r^2 = r_{g*}^2 m^{2/3}$ follows. Then the cross section reads

$$\Sigma(m, m') = \epsilon(v_{\rm rel}/v_g)\pi r_{g*}^2(m^{2/3} + m'^{2/3})[1 + (m^{2/3} + m'^{2/3})v_{g*}^2/v_{\rm rel}^2] , \quad (3)$$

where r_{g*} and v_{g*} are the radius and the three-dimensional internal velocity dispersion of a L_* galaxy, respectively.

2.2. Initial Conditions

We assume the galaxy distribution to be *initially* (after cluster formation and virialization) factorized in a mass distribution $P(m)$ times a King spatial profile, which will be subsequently mixed up by the two-body dynamical evolution. Then

$$N(M, r)_{t=0} = \frac{n_0}{(1 + x^2)^{3/2}} P(m) , \quad (4)$$

where we take for $P(m)$ the Press & Shechter shape $P(m) = m^{a-2}e^{-b^2\delta_c^2 m^{2a}/2}$ (the index a depends on the spectrum of cosmological perturbations and is in the range of 0–0.3 at the scale of galaxy clusters), and where $x = r/r_c$ is the distance from

the cluster center in units of the core radius r_c of the King profile. The constant n_0 is taken so as to yield the total number N_{tot} of galaxies inside the cluster virial radius R_v (from the virial theorem $R_v = GM/3\sigma$); thus,

$$n_0 = \frac{N_{\text{tot}}}{4\pi r_c^3 I_R I_M}, \tag{5}$$

where $I_R \equiv \int_0^{R_v/r_c} dx \ x^2/(1 + x^2)^{3/2}$ and $I_M \equiv \int_0^\infty dm \ P(m)$ are the adimensional integrals of the initial spatial and mass distributions, respectively.

2.3. Numerical Solutions

To integrate equation (2) we first write it in a completely adimensional form for the normalized r-dependent mass distribution $n_t(m, r) \equiv N(m, r, t)/n_0$. We define the adimensional time variable $\tau \equiv t/t_{\text{cr}} \approx 2 \cdot 10^9 \ \text{yr} \ (R_v/1 \ \text{Mpc})(\sigma/10^3 \ \text{km s}^{-1})^{-1}$
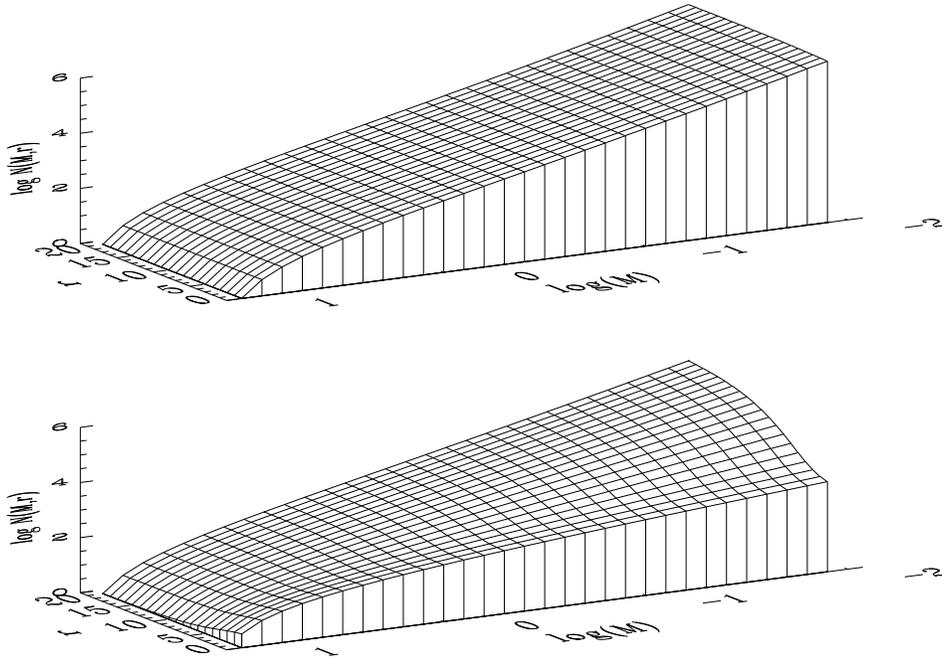
FIG. 1.—Position-dependent mass distribution obtained from the solution of equation (6) for a cluster with the parameters given in the text (arbitrary units are used for r and M). Top panel shows the initial condition, while the bottom panel shows the evolved distribution at $t = 5t_{\text{cr}}$. Note the flattening at the low-mass end in the central region.
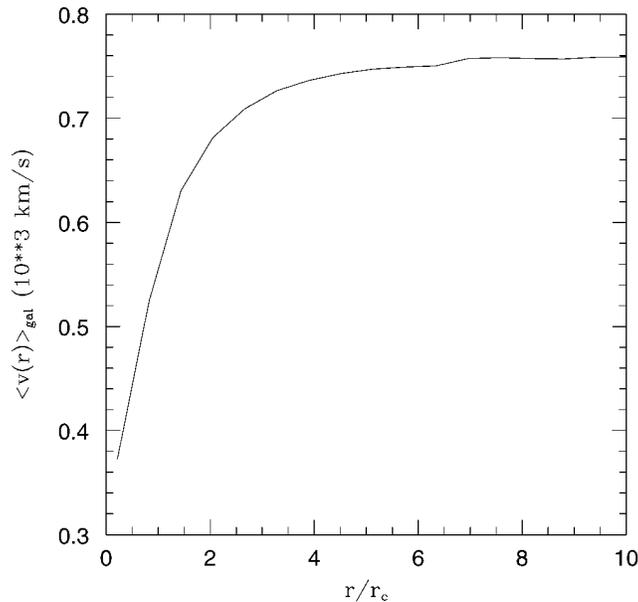
FIG. 2.—Corresponding integrated velocity dispersion, calculated as shown in Paper II. Note the decrease toward the central region, corresponding to the loss of orbital energy by aggregations occurring in the cluster center.

in terms of the cluster crossing time $t_{cr} \equiv 2R_v/\sigma$. The adimensional velocities $\tilde{v} \equiv v/\sigma$ are normalized to the dark matter velocity dispersion σ. The corresponding adimensional interaction rate $\eta(m, m') = n_0 \Sigma R_v \tilde{v}$ can be computed from equations (3) and (4). Then the Smoluchowski equation for the normalized mass distribution $n_\tau(m, r) \equiv N(M, r, \tau)/n_0$ can be recast in the form

$$\partial_\tau n_\tau(m, r) = \tfrac{1}{2} \int_0^m dm' n_\tau(m', r) n_\tau(m-m', r) \langle \eta(m', m-m') \rangle - \int_0^m dm' n_\tau(m, r) n_\tau(m', r) \langle \eta(m, m') \rangle , \tag{6a}$$

$$\eta(m, m') = \frac{1}{2} \frac{R_v}{r_c} \frac{r_{g*}^2}{r_c^2} \frac{N_{tot}}{I_R I_M} \tilde{v}_{rel} (m^{2/3} + m'^{2/3}) \left[\frac{1 + (m^{2/3} + m'^{2/3}) \tilde{v}_{g*}^2}{\tilde{v}_{rel}^2} \right] . \tag{6b}$$

From equation (6) it is evident that for a constant R_v/r_c ratio, the effect of aggregation is larger for clusters with a small core radius (galaxies in the center more concentrated) and with a larger number of galaxies N_{tot}.

The average of the aggregation rate in equation (6b),

$$\langle \eta \rangle \equiv \int d\alpha \int_0^{|\tilde{\boldsymbol{v}}_1 - \tilde{\boldsymbol{v}}_2| = 3\tilde{v}_g} d\tilde{v}_1 \, \tilde{v}_1^2 \, p(\tilde{v}_1) d\tilde{v}_2 \, \tilde{v}_2^2 \, p(\tilde{v}_2) \eta \left(\frac{|\tilde{\boldsymbol{v}}_1 - \tilde{\boldsymbol{v}}_2|}{\tilde{v}_g} \right) , \tag{7}$$

is over the velocities $\tilde{v}_1$ and $\tilde{v}_2$, normalized to the dark matter velocity dispersion σ, of galaxies colliding with relative angle α; the condition $|\tilde{\boldsymbol{v}}_1 - \tilde{\boldsymbol{v}}_2| \leq 3\tilde{v}_g$ accounts for the efficiency $\epsilon(v_{rel}/v_g)$. We assume the distribution of velocities $p(\tilde{v}) = (1/2\pi)^{-3/2} e^{-\tilde{v}^2/2}$ to be Gaussian, as expected after violent relaxation (Lynden-Bell 1967). Note that for clusters with $\sigma \lesssim 900$ km s^{-1}, equation (7) yields significant averaged aggregation rates $\langle \eta \rangle$, assuming a three-dimensional internal velocity dispersion $v_{g*} = 300$ km s^{-1} for an L_* galaxy with $r_{g*} = 60 \, h^{-1}$ kpc.[1] The adopted value of v_{g*} corresponds to a circular velocity of ≈ 220 km s^{-1}; such a value is consistent with that derived from the Faber-Jackson relation for an L_* galaxy, and with the measurements of Tonry & Davis (1981), Dressler (1984), and Dressler et al. (1987). The adopted value of r_{g*} (which refers to the dark halo of an L_* galaxy) is a conservative one, when compared with observational results from absorption lines measured by Steidel (1995), Lanzetta et al. (1995), and Barcons, Lanzetta, & Webb (1995).

Equation (6) is integrated up to $\tau = 5$, with time increments of $\Delta\tau = 1/500$ and a mass step of $\Delta m = 1/500$, from a minimum mass $m_{min} = 10^{-2}$ to a maximum mass $m_{max} = 10^2$ (integrating up to larger times does not sensitively affect our results). When aggregations are effective, the final mass distribution will be changed from the initial one only in the central core, where the galaxy density is larger and binary aggregations are favored. Thus, in the core larger galaxies will form via binary merging, while the initial mass distribution remains unchanged in the outer regions. The evolution of the mass distribution at different radii in a typical cluster (with $N_{tot} = 1000$, $\sigma = 800$ km s^{-1}, and $r_c = 250 \, h^{-1}$ kpc) is shown in Figure 1. The distribution flattens in the central region as a result of the disappearance of small galaxies, which aggregate to form larger ones. Since aggregations among galaxies cause a loss of orbital kinetic energy, we expect such an effect to correlate with smaller galaxy velocity dispersions in the central regions, i.e., with velocity profiles falling toward the center (as we discussed in Paper II); this is actually the case, as is shown in Figure 2. A further effect is that brighter galaxies (which form mainly in the central, denser regions) will have smaller relative separations. This effect is observed in several clusters, as we discuss in the next section.

The strength of the above effects depends on the cluster properties, which in our model engage only through N_{tot}, σ, and r_c, as is shown by equation (6). For example, for a given N_{tot} and σ, merging will be less effective in clusters with large r_c (see the merging rate in eq. [6b]), because the total number of galaxies is spread out over a larger region.

3. COMPARISON WITH OBSERVATIONS

3.1. Method

In the literature (Capelato et al. 1980; Dominguez-Tenreiro & del Pozo-Sanz 1988), the LS has been quantified in terms of the cross-correlation function

$$\Pi_a(s) = \int_V d\phi d^2 r n_a(r) n_a(r + s) \tag{8}$$

between densities of galaxies separated by a distance s in a given magnitude range $[a]$ (ϕ being the angle between r and s) in a region V. The distance distribution function for pairs in a given class is then given by

$$P_a(s)ds = 2\pi s \, ds \Pi_a(s) . \tag{9}$$

If the position of the peak in the distribution $P(s)$ changes depending on the magnitude class $[a]$, a LS is present. The average separation of galaxies in the magnitude class $[a]$ derived from equation (8) is given by

$$\lambda_a = \frac{\int_0^{S_{max}} ds s P_a(s)}{\int_0^{S_{max}} ds P_a(s)} , \tag{10}$$

where S_{max} is the maximum intergalactic distance. Galaxies belonging to a class $[a]$ will be called "segregated" with respect to those in the class $[a']$ if $\lambda_a < \lambda_{a'}$.

Such an effect has been measured in several clusters (Capelato et al. 1980; Dominguez-Tenreiro & del Pozo-Sanz 1988; Yepes, Dominguez-Tenreiro, & del Pozo-Sanz 1991; Yepes & Dominguez-Tenreiro 1992), and fits to the observed $P(s)$ for different classes of magnitude have been given by the same authors. We consider all the clusters for which such an analysis has

---

[1] In the text, we adopt $h = 0.5$ for the Hubble constant $H_0 = 100h$ km s^{-1} Mpc^{-1}.

been performed except Perseus, whose prominent substructure (Gallagher, Han, & Wyse 1996) makes it too complex to be described in the framework of our model. These are reported in Table 1, together with their core radius, velocity dispersion, and observed number of galaxies inside a distance R_{max}. This table also lists the magnitude ranges [a] for which we compute the correlation function.

To make comparisons with such observational material, we proceed as follows:

1. For each observed cluster, we compute the number of galaxies N_{tot} enclosed inside R_V for the whole mass range $0.01 < M/M_* < 10$ (used in the numerical integration of eq. [6]), corresponding to a luminosity range of $0.01 < (L/L_*)^\gamma < 10$ for $M/L \propto L^{\gamma-1}$ (here we take $\gamma = 1$, but see discussion in § 4 for the effect of changing M/L). In practice, N_{tot} is computed by extrapolating the observed number N_{obs} of galaxies (inside a radius R_{max}, see Table 1) both in space (up to R_v, using a King profile) and in luminosity (for the whole luminosity range discussed above, using a Shechter luminosity function). The resulting N_{tot} is given as an input for the solution of equation (6), together with the cluster core radius r_c and the dark matter velocity dispersion σ. The latter is derived from observed galaxy velocity dispersions (assuming no velocity bias) or, when the latter are not available, from the X-ray temperature $T = (\mu m_H/k\beta)\sigma^2$ (when measures of β are not available, we shall assume $\beta = 1$). The resulting values (with the references to the corresponding observations) are given in Table 1. The reported σ are affected by uncertainties of $\Delta\sigma/\sigma < 20\%$, due to intrinsic errors in the measurements of velocity dispersions or X-ray temperatures and (when the estimate of σ is obtained from T with no available measurements of β) to the indetermination of β. However, we stress that errors in σ (as well as those in N_{obs}) do not sensitively affect the LS effects resulting from our model. A quantitative discussion of the effect of variations of all the input parameters is given in § 3.3.

2. For each cluster, the r-dependent mass distribution is found by numerically integrating equation (6).

3. We divide the computed mass distribution at each radius according to the classes of apparent magnitudes (see Table 1) that have been used in the analyses of Capelato et al. (1980), Dominguez-Tenreiro & del Pozo-Sanz (1988), Yepes et al. (1991), and Yepes & Dominguez-Tenreiro (1992). To pass from magnitude to mass ranges, we use the M/L ratio discussed above.

4. We compute the distance distribution $P(s)$ resulting from our model and compare it with the fit to observational results found in the literature. For each cluster, the average separation λ_a corresponding to $P_a(s)$ is computed for all the magnitude classes [a] and compared with the observed values.

When the cluster characteristics are such as to make aggregations effective, larger galaxies form preferentially in the central, denser regions (see § 2 and Fig. 1), where the intergalactic separations are smaller. In this case, the distributions $P_a(s)$ will peak

TABLE 1

ANALYZED CLUSTERS OF GALAXIES

Cluster Name	z	r_c	R_{max}	N_{obs}[a]	σ[b]	Group	Magnitude Range[c]
A1758	0.28	0.72	1.25	320	1000	1	$18.09 \leq m_F \leq 20.10$
						2	$20.10 \leq m_F \leq 20.90$
						3	$20.90 \leq m_F \leq 21.70$
A2111	0.23	0.94	1.08	269	970	1	$17.43 \leq m_F \leq 19.43$
						2	$19.43 \leq m_F \leq 20.21$
						3	$20.21 \leq m_F \leq 21.00$
A2218	0.171	0.43	0.87	306	800	1	$17.12 \leq m_f \leq 19.12$
						2	$19.12 \leq m_f \leq 20.15$
						3	$20.15 \leq m_f \leq 21.18$
A2670	0.076	0.198	0.59	220	600	1	$15.40 \leq m_b \leq 18.00$
						2	$18.00 \leq m_b \leq 19.00$
						3	$19.00 \leq m_b \leq 20.00$
Coma.............	0.023	0.3	1.3	400	810	1	$11.80 \leq m_{25} \leq 14.50$
						2	$14.50 \leq m_{25} \leq 15.50$
						3	$15.50 \leq m_{25} \leq 16.50$
						4	$16.50 \leq m_{25} \leq 17.50$
Fornax	0.005	0.36	0.73	68	320	1	$10.20 \leq m_B \leq 13.50$
						2	$13.50 \leq m_B \leq 15.50$
						3	$15.50 \leq m_B \leq 16.50$
0004.8–3450......	0.114	1.20	1.87	333	805	1	$16.32 \leq m_B \leq 19.00$
						2	$19.00 \leq m_B \leq 20.00$
						3	$20.00 \leq m_B \leq 21.00$

[a] Total number of plate galaxies in the circular region of radius R_{max}.

[b] The values in the Table, used as inputs in our model, are derived as described in the text from the following observational material: A1758: $T = 7$ keV and $T = 8$ keV (two clumps) from Ebeling et al. (1996), corresponding to $\sigma = 1000$–1200 km s^{-1}, assuming $\beta = 1$. A2111: $T = 6$ KeV from Wang & Stocke (1993) yields $\sigma = 970$ km s^{-1}, assuming $\beta = 1$. A2218: Direct estimates from Girardi et al. (1997) give $\sigma = 700$–800 km s^{-1}. A2670: $T = 3.9$ keV from David et al. (1993) yields $\sigma = 600$ for $\beta = 0.6$ (Jones & Forman 1984). Coma, Fornax, and 004.8–3450 (also referred to as A2721): direct estimates from Fadda et al. (1996).

[c] Original references for photometric data: for A1758, A2111, and A2218: Butcher, Oemler, & Wells 1983; for A2670: Sharples, Ellis, & Gray 1988; for Fornax: Ferguson 1989; for 0004.8–3450: Carter 1980; for Coma: Godwin & Peach 1977.

at smaller separations for brighter magnitude ranges [a]. Such shifts of the peak with [a] can be expressed by the ratio

$$b_\lambda \equiv \lambda_1/\lambda_3 \tag{11}$$

of the average distances of the brightest class to that of the faintest class.

3.2. Results

The distributions $P_a(s)$ for the different clusters are shown in Figure 3. Table 2 shows the ratio b_λ for our predictions and for the corresponding observations. The agreement with observations is remarkable. The different degrees of segregation (expressed by values $b_\lambda < 1$) observed in the sample are well accounted for by our merging model, and are directly related to the cluster characteristics as follows: for a given total number of galaxies N_{tot}, clusters with small core radii have denser central regions, so that aggregations are more effective and segregation is enhanced. The lack of LS in A2111 can be explained by the presence a large core radius coupled with a limited total number of galaxies. As a confirmation of such an interpretation, we observe that more pronounced segregation takes place in A2670, which has the smallest core radius in the sample. However, LS can occur also in clusters with large r_c if the total number of galaxies N_{tot} is large enough or if σ is very low. In fact, the cluster 0004.8–3450 shows a significant LS with $N_{tot} \simeq 2000$, while the segregation in the Fornax cluster is mostly due to its very low velocity dispersion, $\sigma = 320 \text{ km s}^{-1}$.
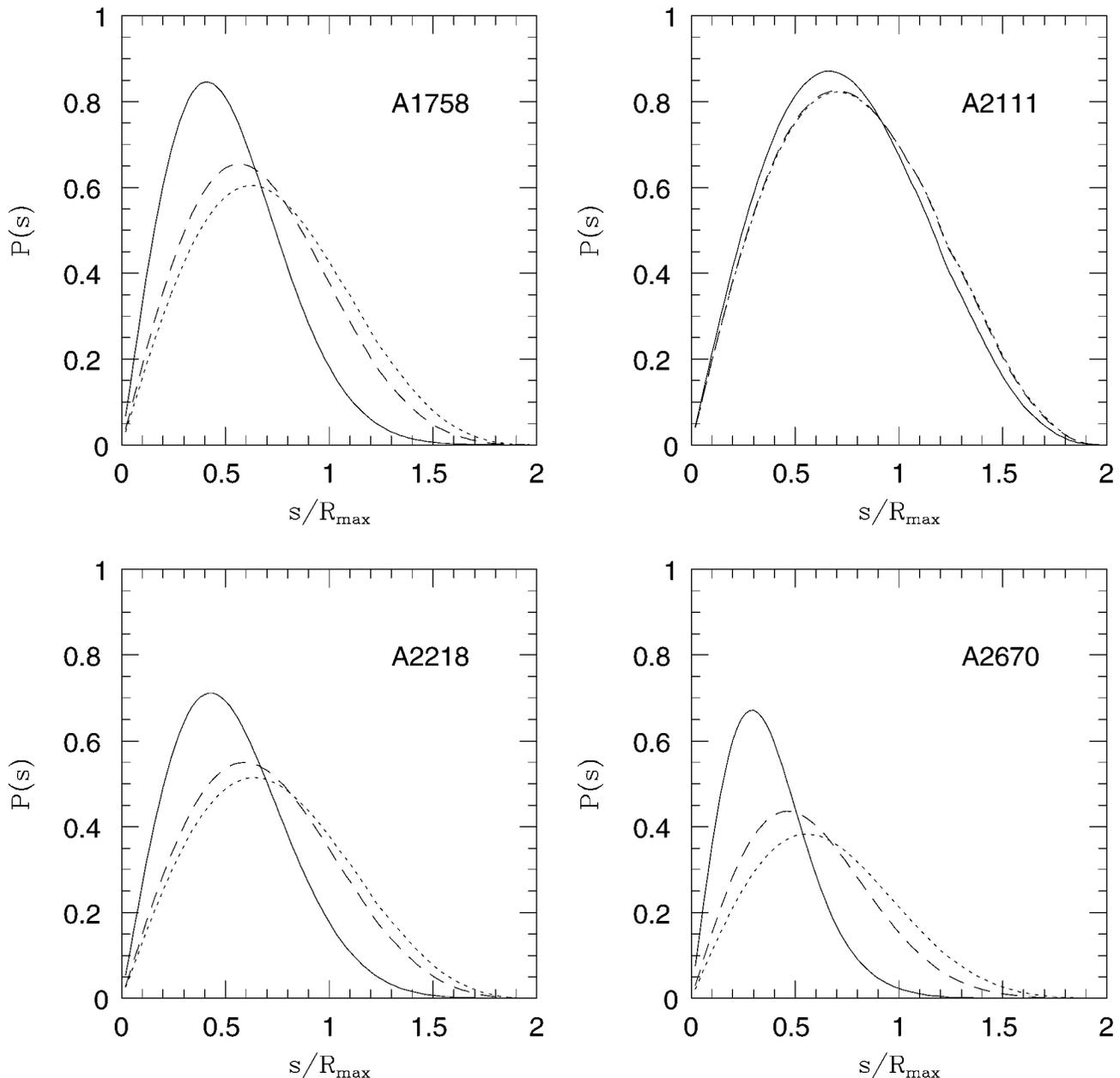
FIG. 3.—Computed intergalactic distance distribution for the clusters with parameters listed in Table 2. Solid curve shows the brighter magnitude class; dotted line shows the fainter. All curves have been computed for a constant M/L.
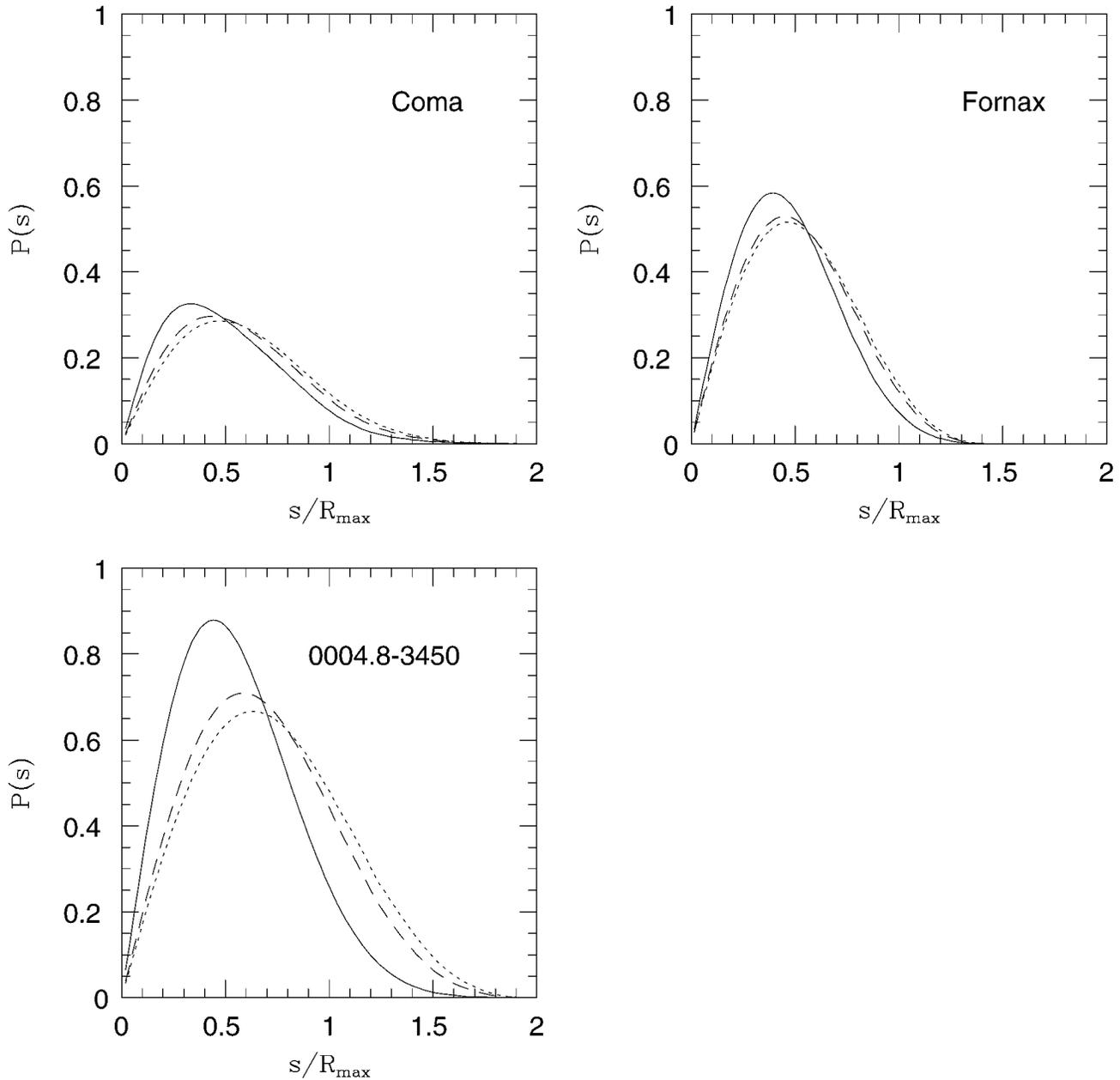
FIG. 3—*Continued*

Note the peculiarity of cluster A2218. The model is in very good agreement for the observed LS of the two brightest magnitude classes with respect to the third one. However, the real data show that the two brightest classes have an antisegregation between them that is not accounted for by our model. We attribute such a mismatch to substructures or anisotropies that our model (based on the schematic assumption of isotropy) cannot reproduce. In fact, recent analysis (Squires et al. 1996) of A2218 indicates the presence of collisions of subclumps, with associated elongated structures in the plasma disposition.

As observed above, our model predicts that the aggregating galaxies will lose part of their kinetic energy. The brightest galaxies in a cluster showing segregation are then expected to have velocity dispersion profiles that decrease toward the center, where the larger density favors aggregations. The computed results for galaxies belonging to magnitude classes 1 and 2 in A2670 (see Fig. 4) confirm this expectation, and are consistent with the available data for such a cluster (Sharples et al. 1988; see also Yepes & Dominguez-Tenreiro 1992). The same calculation for A2111 (see Fig. 4) shows no positive gradient in the profiles, which indicatess a lack of luminosity segregation. Actually, both effects are tightly connected in our model.

3.3. *Varying the Input Parameters*

Here we discuss the effects of varying the input parameters with respect to the reference values in Table 1. The segregation parameter b_λ decreases (indicating larger segregation) for increasing N_{obs} and for decreasing σ and r_c (i.e., for increasing

TABLE 2
LENGTH SCALES

Cluster Name	b_λ (observed)	b_λ (model)
A1758	0.80	0.78
A2111	0.94	0.96
A2218	0.85	0.78
A2670	0.55	0.56
Coma.............	0.83	0.87
Fornax	0.88	0.89
0004.8–3450......	0.85	0.77

NOTE.—Errors in the observed length scales are
<20%. For errors in the model values, see § 3.3.
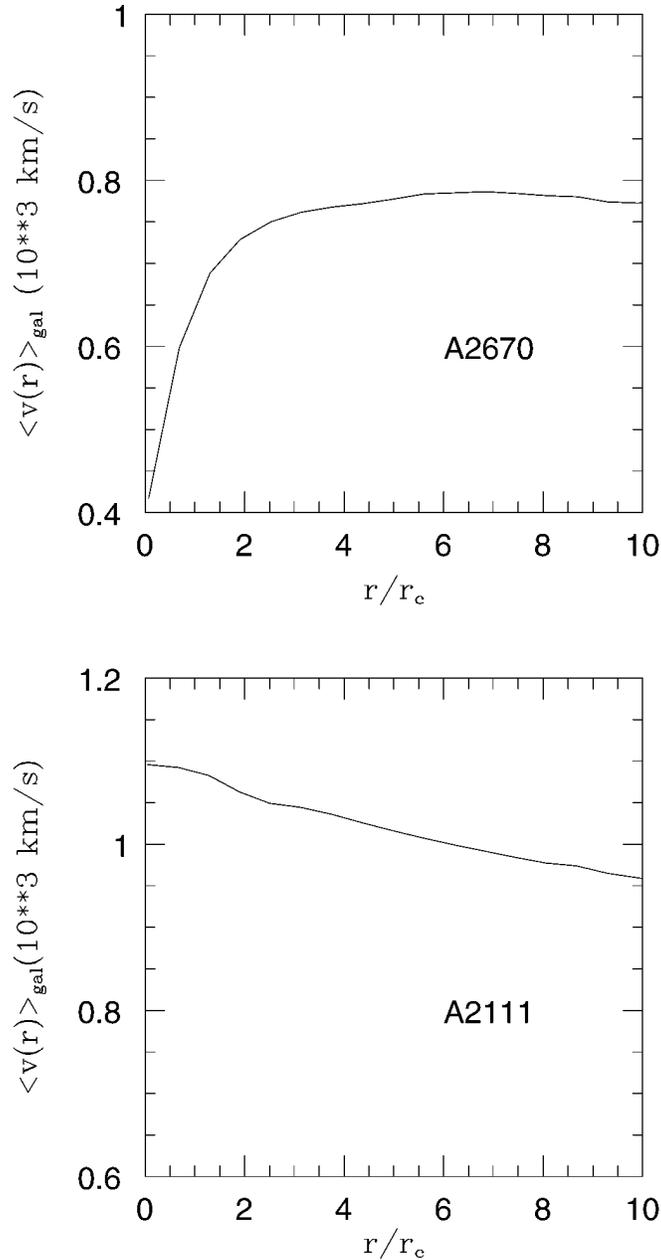
FIG. 4.—Integrated velocity dispersion profiles, computed as shown in Paper II, for the clusters A2670 and A2111

merging efficiency). However, the variations with N_{obs} and σ are very mild. This makes our results robust with respect to the errors associated with those parameters: a 20 % error in N_{obs} or σ results in $\Delta b_\lambda / b_\lambda < 3\%$. The errors in r_c are more important: $\Delta r_c / r_c = 20\%$ yields $\Delta b_\lambda / b_\lambda < 12\%$.

The results for LS do depend on the M/L ratio, which for the sake of simplicity we assumed to be constant. However, the main results presented here also hold for $M/L \propto L^{\gamma-1}$, with $3/4 \leq \gamma \leq 4/3$. This is illustrated in Figure 5, where we show the

distance distribution functions (for the parameters of cluster A2670) derived from the same dynamics (i.e., with the same mass segregation), but with $\gamma = 3/4$ and $\gamma = 4/3$.

4. CONCLUSIONS

We have shown that a detailed model for the dynamics of galaxies aggregating in the potential wells of clusters predicts luminosity segregation (LS) effects of the kind observed in real clusters. The correlation of the strength of the effect with the properties of the clusters predicted in our model is in agreement (see Fig. 3 and Table 2) with that observed for the limited sample of clusters for which LS has been subject to accurate quantitative measurements. In particular, we predict that the effectiveness of aggregations, and hence the degree of LS, will be directly correlated with the number of galaxies in the cluster and inversely correlated with the core radius and with the velocity dispersion (see eq. [6b]).

The results do not depend on the details of the initial mass distribution of galaxies in clusters, which we assume to have a Press & Shechter form with spectral parameter $a = -2$; this independence is the result of the properties of the asymptotic solution of the Smoluchowski equation (describing the evolution of the position-dependent galaxy mass function in our model) and can be traced back to the nonlinear nature of such equations.

Our results are robust with respect to uncertainties in the input quantities and the adopted $L(M)$, as shown in § 3.3. As for our assumption of fixed galaxy velocity distribution, this does not hold when aggregations are effective (see Papers I and II).
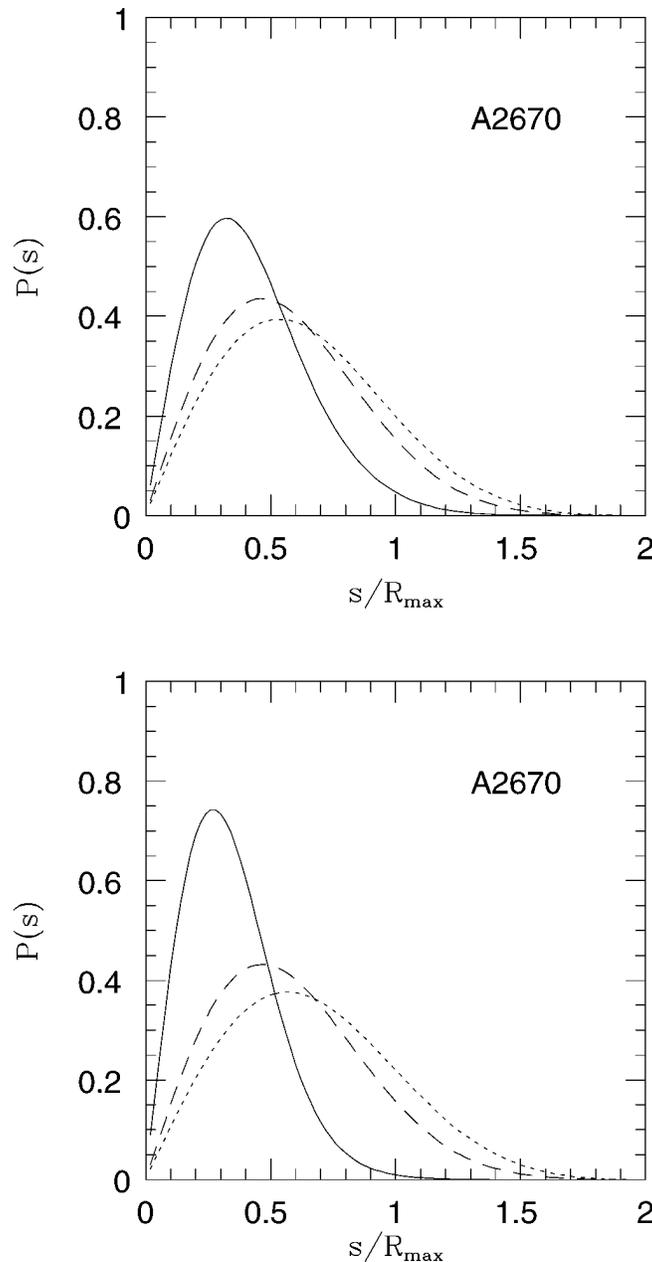
FIG. 5.—Computed intergalactic distance distribution for the cluster A2670 for different values of the $M/L \propto L^{\gamma-1}$ ratio (see text). Top panel shows $\gamma = 3/4$, bottom panel shows $\gamma = 4/3$.

However, the merging-induced shift of $\sim 10\%$–15% of the velocity dispersion toward smaller values *increases* the efficiency of aggregations, so that our assumption is actually conservative. We have rerun our computation for shifted velocity distributions and find results almost indistinguishable from those presented here. Finally, we stress that no attempt at parameter optimization has been made. An even better agreement could be found if the cluster parameters were suitably tuned.

As for the big picture of the evolution of clusters in the two-body dynamical phase, our model focuses on the effects of inelastic collisions not considered in previous works on this subject. In particular, the Fokker-Planck approach of Yepes & Dominguez-Tenreiro (1992) only considers elastic collisions by means of a mean field approximation, with input parameters chosen from a grid of models to show that, within the set of models, it is possible to match the observed segregation effects.

Here we solve the collisional Boltzmann equation, including inelastic collisions, using the *measured* values for input model parameters. Although the latter are subject to errors, we showed (in § 3.3) that the model is robust to uncertainties of $<12\%$ in the parameters. Our results show that inelastic collisions produce appreciable dynamical effects for clusters with one-dimensional velocity dispersions of $\lesssim 900$ km s^{-1}. Such effects show up in different but connected observables: the velocity bias (due to the *average* loss of kinetic energy in inelastic collisions) $b_v \approx 0.8$–0.9 can be observed in X-rays in the form of the β-parameter (see Cavaliere & Fusco-Femiano 1976) $\beta = b_v^2 < 1$; centrally rising velocity dispersion profiles (due to the *differential* loss of kinetic energy at different radii) are now being measured with great accuracy in the optical (Girardi et al. 1996); and different average separations of massive galaxies with respect to faint ones, $b_\lambda \approx 0.8$–0.9 (see eq. [5]), i.e., luminosity segregation (due to the differential mass growth from aggregations at different radii), have been measured in different clusters (see references cited in this paper).

We note that when interpreted in terms of merger-driven evolution, *all* the above effects are predicted to have the *same* dependence on the cluster parameters, i.e., to be larger for clusters with smaller core radii r_c and galaxy velocity dispersions σ, although the strength of the σ-dependence is mild for LS effects.

The observational tests for such predictions are critically affected by the presence of clusters with anisotropies and/or substructures in the observational sample. An inverse correlations of the $\beta < 1$ effect with r_c has been found by, e.g., Jones & Forman (1984), while the anticorrelation with σ has been pointed out by Kriss et al. (1983), Jones & Forman (1984), Edge & Stewart (1991), Bird, Mushotzky, & Metzler (1995), and Jones et al. (1997), but has not been confirmed by the analyses of Lubin & Bahcall (1993) or Girardi et al. (1996).

For velocity dispersion profiles that decrease toward the center, the observational situation is still unclear. An anticorrelation with σ has been inferred (see Paper II) from the analysis by Girardi et al. (1996) of a sample of 37 clusters, when clusters with prominent substructures are excluded; however, the detection of such a correlation in the data (see also den Hartog & Katgert 1996) is made difficult by the presence of anisotropies and/or substructures, which can hurt or destroy the effect of the inelastic collision in the two-body relaxation phase.

As for the LS, the mild (inverse) dependence of the LS effect on σ from merging makes it difficult to observe such a correlation. However, in our model, the strong inverse correlation of LS with r_c predicted by our model is confirmed by the data analysis of Yepes et al. (1991) on the very limited sample of clusters. LS data for a larger sample of clusters with measured r_c would definitely clarify the issue.

Finally, we note that the correlations between different but connected observables predicted by the aggregation model make it testable at the present stage of observational capabilities. Further observational progress (in particular in measuring in detail the velocity dispersion profiles and X-ray temperatures) could definitely probe the predictions of the merging picture, thus assessing the role of aggregations in the dynamical evolution of clusters.

REFERENCES

Barcons, X., Lanzetta, K. M., & Webb, J. K. 1995, Nature, 376, 321
Binngeli, B., Tammann, G. A., & Sandage, A. 1987, AJ, 94, 251
Bird, C. M., Mushotzky, R. F., & Metzler, C. A. 1995, ApJ, 453, 40
Butcher, H., Oemler, A., & Wells, D. C. 1983, ApJS, 52, 183
Capelato, H. V., Gerbal, D., Mathez, G., Mazure, A., Salvador-Solé, E., & Sol, H. 1980, ApJ, 241, 521
Carlberg, R. G. 1994, 433, 468
Carlberg, R. G., & Dubinski, J. 1991, 369, 13
Carter, D. 1980, MNRAS, 190, 307
Cavaliere, A., & Fusco-Femiano, R. 1976, A&A, 49, 137
Cavaliere, A., & Menci, N. 1993, ApJ, 407, L9
David, L. P., Slyz, A., Jones, C., Forman, W., Vrtilek, S. D., & Arnaud, K. A. 1993, ApJ, 412, 479
den Hartog, R., & Katgert, P. 1996, MNRAS, 279, 349
Dominguez-Tenreiro, R., & del Pozo-Sanz, R. 1988, ApJ, 324, 677
Dressler, A. 1978, ApJ, 226, 55
———. 1984, ApJ, 281, 512
Dressler, A., Lynden-Bell, D., Burstein, D., Davies, R. L., Faber, S. M., Terlevich, R. J., & Wegner, G. 1987, ApJ, 313, 42
Ebeling, H., Voges, W., Boheringer, H., Edge, A. C., Huchra, J. P., & Briel, U. G. 1996, MNRAS, 281, 799
Edge, A. C., & Stewart, G. C. 1991, MNRAS, 252, 414
Evrard, A. E., Summers, F. J., & David, M. 1994, ApJ, 422, 11
Fadda, D., Girardi, M., Giuricin, G., Mardirossian, F., & Mezzetti, M. 1996, ApJ, 473, 670
Farouki, R. T., Hoffman, G. L., & Salpeter, E. E. 1983, ApJ, 271, 11

Ferguson, H. C. 1989, AJ, 98, 367
Fusco-Femiano, R., & Menci, N. 1995, ApJ, 449, 431 (Paper I)
Gallagher, J. S., III, Han, M., & Wyse, R. F. G. 1996, BAAS, 188, 06.08
Girardi, M., Fadda, D., Escalera, E., Giuricin, G., Mardirossian, F., & Mezzetti, M. 1997, preprint astro-ph/9707098
Girardi, M., Fadda, D., Giuricin, G., Mardirossian, F., Mezzetti, M., & Biviano, A. 1996, ApJ, 457, 61
Godwin, J. G., & Peach, J. V. 1977, MNRAS, 181, 323
Katz, N., & White, S. D. M. 1993, ApJ, 412, 455
Kent, S. M., & Gunn, J. E. 1982, AJ, 87, 945
Kent, S. M., & Sargent, W. L. 1983, AJ, 230, 667
Kriss, G., Cioffi, D., & Canizares, C. 1983, ApJ, 272, 439
Jones, C., David, L., Forman, W., Churasov, E., & Gilfanov, M. 1997, CfA preprint 4471
Jones, C., & Forman, W. 1984, ApJ, 276, 38
Lanzetta, K. M., Bowen, D. V., Tytler, D., & Webb, J. K. 1995, ApJ, 442, 538
Lubin, L. M., & Bahcall, N. B. 1993, ApJ, 415, L27
Lynden-Bell, D. 1967, MNRAS, 136, 101
Menci, N., & Fusco-Femiano, R. 1996, ApJ, 472, 46 (Paper II)
Oegerle, W. R., Hoessel, J. G., & Ernst, R. M. 1986, AJ, 91, 4
Oemler, A. 1974, ApJ, 194, 1
Quintana, H. 1979, AJ, 84, 15
Richstone, D. O., & Malmuth, E. M. 1983, ApJ, 268, 30
Rood, H. J., Page, T. L., Kintner, E. C., & King, I. 1972, ApJ, 175, 627
Roos, N., & Aarseth, S. I. 1982, A&A, 114, 41

Sarazin, C. L. 1980, ApJ, 236, 75
Saslaw, W. C. 1985, Gravitational Physics of Stellar and Galactic Systems (Cambridge: Cambridge Univ. Press)
Sharples, R. M., Ellis, R. S., & Gray, P. M. 1988, MNRAS, 231, 479
Squires, G., Kaiser, N., Babul, A., Fahlman, G., Woods, D., Neuman, D. M., & Böhringer, H. 1996, ApJ, 461, 572
Steidel, C. C. 1995, in QSO Absorption Lines, ed. G. Meylan (Berlin: Springer), 135

Stein, P. 1996, preprint astro-ph/9606162
Summers, F. J., Davis, M., & Evrard, A. E. 1995, ApJ, 454, 1
Tonry, J. L., & Davis, M. 1981, ApJ, 246, 680
Wang, Q., & Stocke, J. T. 1993, ApJ, 408, 71
White, S. D. M. 1977, MNRAS, 179, 33
Yepes, G., & Dominguez-Tenreiro, R. 1992, ApJ 387, 27
Yepes, G., Dominguez-Tenreiro, R., & del Pozo-Sanz, R. 1991, ApJ, 373, 336